Macromolecules

Article

pubs.acs.org/Macromolecules

Self-Assembly of Binary Mesocrystals from Blends of BABCB Multiblock Copolymers and ABC Triblock Copolymers

Meijiao Liu,[†] Binkai Xia,[†] Weihua Li,*[,†] Feng Qiu,[†] and An-Chang Shi[‡]

[†]State Key Laboratory of Molecular Engineering of Polymers, Collaborative Innovation Center of Polymers and Polymer Composite Materials, Department of Macromolecular Science, Fudan University, Shanghai 200433, China

[‡]Department of Physics and Astronomy, McMaster University, Hamilton, Ontario, Canada L8S 4M1

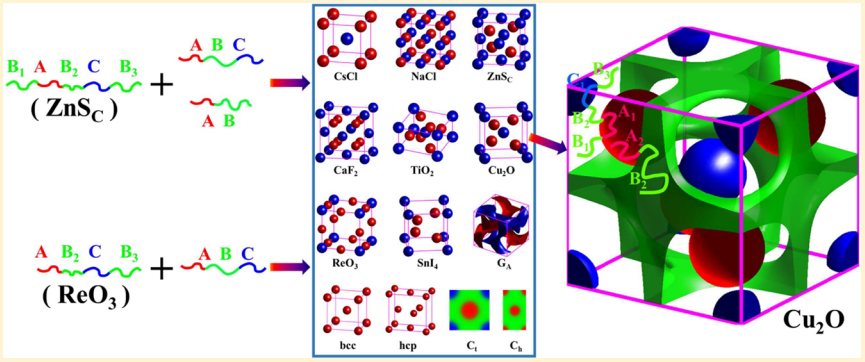

ABSTRACT: The phase behavior of binary blends composed of BABCB-type pentablock terpolymers and ABC-type triblock copolymers is investigated using the self-consistent field theory in the grand canonical ensemble. Specifically, the study is focused on how the simpler copolymers regulate the phase behavior of two sphere-forming multiblock copolymers of the type $B_1AB_2CB_1$ and AB_2CB_3. For certain compositions, these two multiblock copolymers self-assemble to form mesocrystalline phases composed of binary A and C spheres with the ZnS_C and ReO_3 structures, respectively. It is discovered that the addition of symmetric ABC triblocks or AB diblocks to the two multiblock copolymers leads to the formation of different binary crystalline phases including symmetric binary crystalline phase of NaCl type for the A/C-component symmetric blends and asymmetric Cu_2O, SnI_4, TiO_2, and CaF_2 phases for the A/C-component asymmetric blends. In particular, the binary mesocrystals of the Cu_2O and SnI_4 structures observed in the blends of the tail-symmetric $B_1AB_2CB_1$ terpolymers and the AB diblock copolymers are new stable phases which have not been observed in the $B_1AB_2CB_3$ terpolymers melts. The theoretical results demonstrate that blending of block copolymers with specially designed multiblock terpolymers could provide an efficient route to fabricate binary mesocrystals.

INTRODUCTION

Self-assembly of block copolymers, which are macromolecules composed of two or more chemically distinct polymer chains covalently jointed together by their ends, has attracted tremendous research attention due to their ability to form very rich nanostructured ordered microphases.[1−4] The symmetry and stability of these ordered phases are determined by the molecular properties of the block copolymers and the interactions between the different blocks. For AB diblock copolymer, which is the simplest block copolymer, its phase behavior is largely dictated by two parameters, i.e., the volume fraction of the A block f and the immiscibility degree characterized by the product χN, where N is the total number of statistical segments of the polymer and χ is the Flory−Huggins interaction parameter characterizing the AB integration. It is amazing that even the simple AB diblock copolymer can self-assemble into a number of ordered phases including lamella, cylinder, bicontinuous network (gyroid and *Fddd*), and sphere.[5−10] The ordered phases from block copolymers have unique properties enabling distinct applications in various fields. For example, the lamellae, hexagonally packed cylinders, and double-gyroid structures self-assembled from high-molecular-weight block copolymers could be used to design one-dimensional (1D),[11] 2D,[12] and 3D[13] photonic crystals. As another example, due to its unique bicontinuous feature, the double-gyroid structure provides an appealing candidate for applications that require bicontinuous nanochannels to facilitate transport phenomena, such as catalysis template, polymer solar cells, and nanoporous membranes.[14−16] Furthermore, one of the most promising applications of block copolymers is in the development of patterning techniques utilizing directed self-assembly (DSA) of block copolymers. The DSA method combines the advantages of traditional lithographic techniques and the self-assembling ability of block copolymers on the length scale of 5−100 nm. This new bottom-up patterning method of DSA with high-resolution and

Received: March 12, 2015
Revised: April 12, 2015
Published: May 6, 2015

DOI: 10.1021/acs.macromol.5b00529
Macromolecules 2015, 48, 3386−3394

high-throughput at a low cost has been successfully applied to fabricate defect-free geometrically simple patterns, i.e., cylinders (dots)[17] or lamellae (stripes),[18] for both fundamental research interest and practical application in the fabrication of high-density storage media and other devices.[19,20] Moreover, DSA has also been used to fabricate some device-orientated irregular structures targeting the manufacture of integrated circuits.[21−23]

Among the various ordered phases self-assembled by block copolymers, the spherical phases, in which spherical microdomains are arranged on crystalline lattices, are particularly interesting because they represent mesoscopic analogues of atomic crystals, e.g., metallic alloy crystals and ionic crystals with exceptional mechanical, electronic, and optical properties. First of all, the self-assembly of sphere-forming block copolymers provides a route for the fabrication of crystalline structures with a feature size of nanometers that can be readily tuned by the molecular weight of block copolymers. These mesocrystals could satisfy a wide range of application needs, such as lithographic templates of high-density magnetic storage media, quantum dots, photonic crystals, and catalysis scaffolds.[24−27] These crystalline structures of spherical phases bridge the gap of feature sizes between the hard atomic crystals and soft mesocrystals self-assembled by spherical colloids with purposely tailored steric interaction potential. Furthermore, the spherical phases offer an ideal model system for the study of the packing of soft spheres on various crystalline lattices, which is a research topic attracting long-lasting interest.[28−36] The packing of spherical domains self-assembled by block copolymers is similar to, but also with significant differences from, two well-known packing problems, i.e., the purely entropy-dominated hard spheres and the interface-optimized equal-sized bubbles (i.e., Kelvin problem), which have been commonly accepted to adopt the crystalline lattices of hexagonal close packing (hcp) and A15, respectively.[37,38] For instance, the stable spherical phase formed by simple asymmetric diblock copolymers with uniform conformational parameter (or segment size) is the body-centered-cubic (bcc) phase except for the hcp phase in a tiny region at the extreme vicinity of the order−disorder transition (ODT).[7]

Compared with atomic crystals, an apparent disadvantage of the self-assembled spherical phases from block copolymers is that only a very limited types of crystalline lattices have been be observed. Extending the repository of spherical phases self-assembled from block copolymers using specifically designed chain architectures is a fascinating but also challenging problem. On the one hand, the vast library of block copolymer architectures offers unparalleled opportunities for tailoring the self-assembly of block copolymers into various spherical phases. On the other hand, the complexity of the system makes the searching of possible phases formed from multiblock copolymers a formidable task.[39] To this end, experimental and theoretical studies have resulted in a few useful design principles which have been validated for the formation of desired spherical phases. For example, for single-component crystalline structures, i.e., the spherical domains formed by the minority component of AB-type block copolymers, the conformational asymmetry, controlled by the size ratio of distinct segments of AB diblock copolymers or by branching the blocks of the major component forming AB_m miktoarm block copolymers, can be used to tune the stable spherical phase from the classical bcc phase to the complex Frank−Kasper σ-phase and the A15 phase.[7,10,40−43] In addition, the complex σ-phase has also been observed in the self-assembly of SISO tetrablock terpolymers by the research group of Bates.[44,45] In another example, one more component is introduced to form three component ABC-type multiblock terpolymers where the two minor components of A and C form spherical domains dispersed in the B-formed matrix and arranged on a binary crystalline lattice. For this system a design principle has been recently proposed, in which the architectures of linear multiblock terpolymers is used to regulate the formation of a large multitude of binary crystalline structures which resemble the symmetries and structures of binary ionic crystals.[4] This design principle can be readily generalized to other topologies of architectures and also to those of tetrapolymers for the formation of ternary crystalline structures. In addition, different design principles can be combined to build up new principles that can lead to the formation of richer spherical phases. These compelling examples demonstrate that designed multiblock copolymers could be used to fabricate rich crystalline structures on the mesoscale.

The basic idea of using multiblock terpolymers for the formation of various binary crystalline phases is to control the packing of spherical domains formed by the two minority (A and C) components by tailoring the majority (B) blocks.[4] For instance, with a tail-symmetric pentablock copolymer of the type $B_1AB_2CB_1$, A and C spherical domains are formed for the minority A and C blocks with equal lengths. The packing of the A and C spheres to a lattice, which is dictated by the effective *bond length* or the coordination number (CN), is then tuned by the relative length of the middle B_2 block while keeping the total B ($= B_1 + B_2 + B_1$) volume fraction constant. As the length of the middle B_2 block decreases, the binary crystalline phase transforms from the CsCl-type lattice to crystals with the NaCl, ZnS sphalerite (ZnS_C), and α-BN structures. Among this transition sequence, the CN decreases from 8 to 6, 4, and 3. When the two tail B blocks become unequal, the asymmetry due to the block copolymer leads to the formation of asymmetric binary crystalline phases, i.e., A and C spheres having unequal CNs. When the block copolymer architecture changes from the tail-symmetric type of $B_1AB_2CB_1$ to the completely tail-asymmetric type of AB_2CB_3, various binary crystalline phases with unequal CNs are formed. From the point of view of fabricating rich binary mesoscale crystals, multiblock terpolymers with different architectures provide a robust platform. However, from a practical point of view, it is technically difficult and expensive in experiments to precisely control the composition and sequence of multiblock terpolymers. An alternative route to synthesizing new block copolymers is to use block copolymer blends and thus to tailor the equilibrium structures by regulating the concentration of one or more species.

In the literature, blending block copolymers or homopolymers together is a widely used method to design new polymeric materials for specific purposes. The simplest blending system is the binary mixture of AB diblock copolymer with A or B homopolymer. Many experimental[46−49] and theoretical[50−53] studies have led to a comprehensive understanding on the phase behavior of AB/A blends. It has been known that the addition of homopolymers can facilitate stabilizing new phases, such as the metastable phases of perforated lamellae (PL) and double diamond (DD) in pure diblock copolymers.[46,51,52] The addition of homopolymers becomes more useful to regulate the effective compositions for stabilizing desired structures in multicomponent polymeric systems, e.g., ABC linear[54,55] or star[56−58] triblock terpolymers.

DOI: 10.1021/acs.macromol.5b00529
Macromolecules 2015, 48, 3386−3394

A number of interesting ordered structures have been obtained by blending ABC triblock terpolymers with their constitutive homopolymers.[54,55] Besides adding homopolymers into block copolymers, blending two or more block copolymers with distinct molecular weights or compositions is another useful scheme to design block copolymer samples for the formation of desired morphologies.[59,60] For instance, the intriguing knitting pattern (KP) morphology was observed in the mixture of two PS−PB−PMMA triblock terpolymers with different lengths of the middle block by Abetz et al.[59] In addition to new ordered structures, blending has been applied to stabilize device-orientated irregular aperiodic structures.[21,61]

In this work, we focus on exploring the phase behavior of various binary mixtures composed of BABCB-type multiblock terpolymer and AB-type diblock or ABC-type triblock copolymer aiming to the fabrication of distinct binary crystalline phases by tuning the concentration of one specific polymer as well as the composition of the simpler block copolymers. Specifically, two linear multiblock terpolymers of the $B_1AB_2CB_3$ type and the AB_2CB_3 type are chosen. In the melt state, these two multiblock copolymers assume a binary crystalline phase with low CN or average CN ($\overline{CN}$), e.g. ZnS_C or ReO_3 structures. On the other hand, it is well-known that the diblock or triblock copolymers usually self-assemble into spherical phases with relative high CN or even nonspherical phases. In a binary mixture composed of the multiblock copolymers and diblock or triblock copolymers, as the concentration of the multiblock terpolymer decreases, a phase transition sequence from the crystalline phase of a low CN to that of a high CN must pass through some crystalline phases with intermediate values of CN, thus providing opportunities for new mesocrystals. In other words, blending of two distinct block copolymers could form new crystalline structures beyond those self-assembled in their respective pure melts.

For a blending system, the phase behavior depends on many parameters, including the concentration of the different species as well as the compositions and interaction parameters of the different blocks. Exploring this large parameter space presents an extremely challenging problem. To this end, theoretical studies could be used to obtain useful insights and guiding principles for the search of complex phases. Note that it is difficult for practical experiments to obtain the morphologies predicted by theoretical calculations in a limited parameter space subject to a highly restricted set of other parameters which cannot be readily targeted at in experiments. However, the understanding on the self-assembling mechanism of complex block copolymer systems and the guiding principle of designing block copolymer materials for targeted structures developed via theoretical calculations are particularly helpful for experiments to obtain interesting structures.

In our study we use the well-developed self-consistent field theory (SCFT)[5,62,63] of polymers to investigate the phase behavior of the block copolymer blends. The SCFT is one of the most successful theoretical methods in the study of block copolymer self-assembly. In particular, it provides an efficient method to determine the phase behavior of polymeric systems because SCFT can be used to compute the free energy of different phases accurately. One obvious weakness of SCFT is neglecting fluctuation effects, which can result in some inaccuracy with the determination of the phase behaviors of real block copolymers.[64] Fortunately, except for the region near the order−disorder transitions, the inaccuracy of SCFT can be safely ignored for polymers with reasonably high molecular weights. Specifically, the pseudospectral method, which solves the SCFT equations by taking advantage of the high efficiency of fast Fourier transformation (FFT), has widely used to explore the phase behavior of various complex block copolymers.[10,65,66] To consider possible macrophase separations in the blending system, we employ the pseudospectral method of SCFT formulated in a grand canonical ensemble to construct the phase diagram of the binary block copolymer blends, aiming to identify the stability regions of distinct crystalline phases as well as their coexisting phase regions. Three typical types of blending systems are considered. The first one is the blend of tail-symmetric pentablock terpolymer $B_1AB_2CB_1$ and symmetric ABC triblock terpolymer, with which a phase transition sequence, from the binary crystalline phase of ZnS_C formed by the pure pentablocks to a new phase of NaCl, and then to CsCl that is stable in the pure triblocks, is expected. In the second blend, the symmetric ABC triblock terpolymer is replaced by an asymmetric AB diblock copolymer, where new binary crystalline phases with unequal CNs are expected to be induced by the A/C-component asymmetry. The third sample is composed of the completely tail-asymmetric tetrablock terpolymer AB_2CB_3 and the symmetrical ABC triblock terpolymer, in which a phase sequence from the binary crystalline phase with unequal CNs to CsCl with equal CN going through various intermediate phases is explored.

THEORY AND METHOD

We consider a generic binary blend of pentablock terpolymer $B_1AB_2CB_3$ and ABC triblock terpolymer. Changing the volume fractions of the different blocks leads to the generation of the three binary blends under consideration. For example, the other two blends, of the pentablock terpolymer $B_1AB_2CB_3$ and AB diblock copolymer, could be obtained by reducing the length of the C block in ABC to be zero and of the tetrablock terpolymer AB_2CB_3 and ABC triblock terpolymer by reducing the length of the B_1 block in $B_1AB_2CB_3$ to be zero. The blend of a volume V consists of n_1 $B_1AB_2CB_3$ terpolymers of total statistical segments N and n_2 ABC terpolymers of γN segments, where γ quantifies the length ratio of the two polymer chains. All polymer chains in the blend are assumed to be incompressible and to have a fixed uniform monomer density ρ_0 and a uniform statistical segment length b. The compositions (or volume fractions) of the two terpolymers are characterized by two groups of volume fractions $f_K^{(1)}$ and $f_K^{(2)}$ with $f_A^{(i)} + f_B^{(i)} + f_C^{(i)} = 1$ ($i = 1, 2$), respectively. For the pentablock terpolymer, the three B blocks are specified by $f_{B_1}^{(1)}$, $f_{B_2}^{(1)}$, and $f_{B_3}^{(1)}$ ($f_{B_1}^{(1)} + f_{B_2}^{(1)} + f_{B_3}^{(1)} = f_B^{(1)}$), respectively. The immiscibility degrees of the three-component blend are given by three interaction parameters, $\chi_{AB}N$, $\chi_{BC}N$, and $\chi_{AC}N$.

The standard SCFT formulation for block copolymers in the canonical[5,50,62,63] or grand canonical[51,67,68] ensemble is described in the literatures. In what follows we reformulate the theory for the binary blending system in the grand canonical ensemble. Note that the numbers of chains, n_1 and n_2, of the two polymers in the grand canonical ensemble are not fixed, and instead, they are regulated by their chemical potentials, μ_1 and μ_2, respectively. Under the incompressibility condition, only one of the two chemical potentials is an independent variable. Without loss of generality, we choose the controlling parameter as μ_2 while setting $\mu_1 = 0$. The free energy of the Gaussian chain model under the mean-field approximation in the unit of thermal energy k_BT, where k_B is

DOI: 10.1021/acs.macromol.5b00529
Macromolecules 2015, 48, 3386−3394

the Boltzmann constant and T is a given temperature, can be expressed as

$$\frac{NF}{\rho_0 k_B T} = -Q_1 - z_2 Q_2 + \int d\mathbf{r}\{\chi_{AB}N\phi_A(\mathbf{r})\phi_B(\mathbf{r}) + \chi_{AC}N\phi_A(\mathbf{r})\phi_C(\mathbf{r}) + \chi_{BC}N\phi_B(\mathbf{r})\phi_C(\mathbf{r}) - w_A(\mathbf{r})\phi_A(\mathbf{r}) - w_B(\mathbf{r})\phi_B(\mathbf{r}) - w_C(\mathbf{r})\phi_C(\mathbf{r}) - \eta(\mathbf{r})[1 - \phi_A(\mathbf{r}) - \phi_B(\mathbf{r}) - \phi_C(\mathbf{r})]\} \quad (1)$$

where $z_2 = \exp(\mu_2/k_BT)$is the activity, and $\phi_K(\mathbf{r})$ (K = A, B, and C) are the monomer densities whose periodic distributions characterize the ordered phase. The field function $\eta(\mathbf{r})$ is a Lagrange multiplier used to enforce the incompressibility conditions, $\phi_A(\mathbf{r}) + \phi_B(\mathbf{r}) + \phi_C(\mathbf{r}) = 1$. The two quantities Q_1 and Q_2 are the single chain partition functions of the two types of terpolymers interacting with the mean fields of $w_K(\mathbf{r})$ (K = A, B, and C), which are produced by surrounding chains and are given by

$$Q_1 = \int d\mathbf{r}\, q_1(\mathbf{r}, s)q_1^\dagger(\mathbf{r}, s) \quad (2)$$

$$Q_2 = \int d\mathbf{r}\, q_2(\mathbf{r}, s)q_2^\dagger(\mathbf{r}, s) \quad (3)$$

Here $q_i(\mathbf{r},s)$ and $q_i^\dagger(\mathbf{r},s)$ (i = 1 and 2) are the end-segment distributions for the two types of polymers, satisfying the following modified diffusion equations

$$\frac{\partial q_1(\mathbf{r}, s)}{\partial s} = \nabla^2 q_1(\mathbf{r}, s) - w(\mathbf{r}, s)q_1(\mathbf{r}, s) \quad (4)$$

$$-\frac{\partial q_1^\dagger(\mathbf{r}, s)}{\partial s} = \nabla^2 q_1^\dagger(\mathbf{r}, s) - w(\mathbf{r}, s)q_1^\dagger(\mathbf{r}, s) \quad (5)$$

$$\frac{\partial q_2(\mathbf{r}, s)}{\partial s} = \nabla^2 q_2(\mathbf{r}, s) - w(\mathbf{r}, s)q_2(\mathbf{r}, s) \quad (6)$$

$$-\frac{\partial q_2^\dagger(\mathbf{r}, s)}{\partial s} = \nabla^2 q_2^\dagger(\mathbf{r}, s) - w(\mathbf{r}, s)q_2^\dagger(\mathbf{r}, s) \quad (7)$$

where $w(\mathbf{r},s) = w_K(\mathbf{r})$ when s belongs to the K-component blocks along the polymer chains. The above expressions imply that $R_g = N^{1/2}b/\sqrt{6}$ is chosen as the length unit, and $s \in [0, 1]$ for the terpolymer $B_1AB_2CB_3$ while $s \in [0, \gamma]$ for the other terpolymer. The initial conditions of the propagator functions are $q_1(\mathbf{r},0) = q_2(\mathbf{r},0) = 1$, $q_1^\dagger(\mathbf{r},1) = 1$, and $q_2^\dagger(\mathbf{r},\gamma) = 1$. Minimization of the free energy with respect to the monomer densities and the mean fields leads to the following SCFT equations

$$w_A(\mathbf{r}) = \chi_{AB}N\phi_B(\mathbf{r}) + \chi_{AC}N\phi_C(\mathbf{r}) + \eta(\mathbf{r}) \quad (8)$$

$$w_B(\mathbf{r}) = \chi_{AB}N\phi_A(\mathbf{r}) + \chi_{BC}N\phi_C(\mathbf{r}) + \eta(\mathbf{r}) \quad (9)$$

$$w_C(\mathbf{r}) = \chi_{AC}N\phi_A(\mathbf{r}) + \chi_{BC}N\phi_B(\mathbf{r}) + \eta(\mathbf{r}) \quad (10)$$

$$\phi_A(\mathbf{r}) = \int_{f_{B_1}^{(1)}}^{f_{B_1}^{(1)}+f_A^{(1)}} ds\, q_1(\mathbf{r}, s)q_1^\dagger(\mathbf{r}, s) + z_2\gamma \int_0^{f_A^{(2)}} ds \times q_2(\mathbf{r}, s)q_2^\dagger(\mathbf{r}, s) \quad (11)$$

$$\phi_B(\mathbf{r}) = \int_0^{f_{B_1}^{(1)}} ds\, q_1(\mathbf{r}, s)q_1^\dagger(\mathbf{r}, s) + \int_{f_{B_1}^{(1)}+f_A^{(1)}}^{f_{B_1}^{(1)}+f_A^{(1)}+f_{B_2}^{(1)}} ds \times q_1(\mathbf{r}, s)q_1^\dagger(\mathbf{r}, s) + \int_{1-f_{B_3}^{(1)}}^{1} ds\, q_1(\mathbf{r}, s)q_1^\dagger(\mathbf{r}, s) + z_2\gamma \int_{f_A^{(2)}}^{f_A^{(2)}+f_B^{(2)}} ds\, q_2(\mathbf{r}, s)q_2^\dagger(\mathbf{r}, s) \quad (12)$$

$$\phi_C(\mathbf{r}) = \int_{1-f_C^{(1)}-f_{B_3}^{(1)}}^{1-f_{B_3}^{(1)}} ds\, q_1(\mathbf{r}, s)q_1^\dagger(\mathbf{r}, s) + z_2\gamma \int_{1-f_C^{(2)}}^{1} ds \times q_2(\mathbf{r}, s)q_2^\dagger(\mathbf{r}, s) \quad (13)$$

The SCFT equations can be solved numerically using a standard iteration scheme. Here we employ the pseudospectral method[69,70] to solve the modified diffusion equations and implement the Anderson mixing iteration scheme[71] to accelerate the converging speed toward SCFT solutions. It has been shown that the pseudospectral method can give reliable accuracy of the free energy for fine grid spacing and step size of the contour length,[72] especially with the fourth-order algorithm.[73,74] In addition, it has been verified that the second-order one is also able to accurately identify the phase transitions in weak or intermediate segregation which is dependent on the relative values of free energy.[75] The binary blend is placed in a rectangular box with periodic boundary conditions in the three directions. The grid spacing is chosen to be smaller than $0.1R_g$, and the discrete step of the chain contours is set up as $\Delta s = 0.005$. Although the calculations are performed in the grand canonical ensemble, we present our results in terms of the canonical variable ϕ_1, where ϕ_1 is the spatial average concentration of the multiblock terpolymer in the blend. ϕ_1 is conjugated to z_2 and γ and can be calculated by

$$\phi_1 = Q_1 = 1.0 - z_2\gamma Q_2 \quad (14)$$

RESULTS AND DISCUSSION

Compared with two-component block copolymer systems, the parameter space of the three-component block copolymer systems is much larger. Even with the assumption of uniform monomer sizes, there are at least five free parameters, including three interaction parameters $\chi_{ij}N$ (i, j = A, B, C) and two independent volume fractions. In the current binary blend of the multiblock terpolymer $B_1AB_2CB_3$ and the ABC triblock terpolymer, a few additional parameters are required to specify the system, i.e., the length ratio γ between the two types of terpolymers, the concentration ϕ_1 and the compositions (e.g., $f_{B_1}^{(1)}$ and $f_{B_2}^{(1)}$) of different B blocks of the $B_1AB_2CB_3$ terpolymer. To focus on the effects of the addition of simpler block copolymers on the phase behaviors of the tail symmetric or asymmetric multiblock terpolymer $B_1AB_2CB_3$ or AB_2CB_3, we first fix all characteristic parameters of the multiblock terpolymer including interaction parameters of $\chi N = \chi_{AB}N = \chi_{BC}N = \chi_{AC}N = 80$ and compositions of $f_A^{(1)} = f_C^{(1)} = 0.11$ and $f_{B_1}^{(1)} = f_{B_3}^{(1)} = 0.34$ for $B_1AB_2CB_3$ and $f_A^{(1)} = f_C^{(1)} = 0.09$ and $f_{B_2}^{(1)} = 0.20$ for AB_2CB_3. With these fixed parameters, the pure melts of the two multiblock terpolymers self-assemble into the binary ZnS_C and ReO_3 phases, respectively. Then we vary the concentration of the multiblock terpolymer ϕ_1 and the composition or the length ratio of the AB diblock or ABC triblock copolymer to examine the two-dimensional cross

DOI: 10.1021/acs.macromol.5b00529
Macromolecules 2015, 48, 3386−3394

section of the full multidimensional phase diagram. Furthermore, the construction of the phase diagrams is carried out by comparing the free energy of various candidate phases of the system. In our SCFT calculation, the candidate phases are shown in Figure 1.

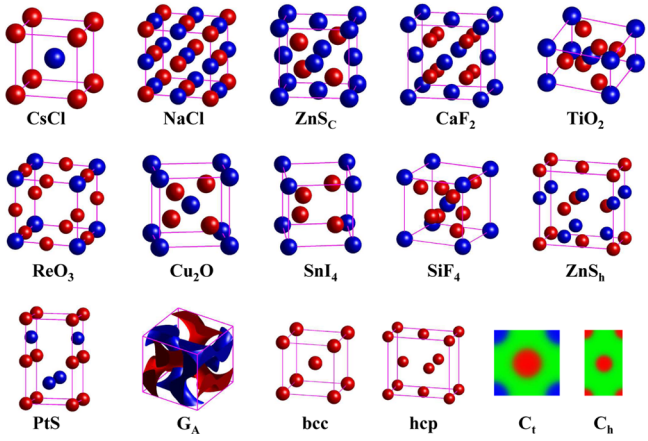

Figure 1. Plots of the candidate 2D and 3D phases considered in this work, where A and C domains in the 2D and 3D plots are indicated by red and blue colors, respectively, while the B domain is not shown in 3D or indicated by green color in 2D.

For the first blend composed of tail-symmetric pentablocks, $B_1AB_2CB_1$, and symmetric ABC triblocks with a fixed length ratio $\gamma = 0.5$, the 2D cross section of the phase diagram with respect to the volume fraction $f_A^{(2)} = f_C^{(2)}$ of the two end blocks of the ABC triblocks and the concentration of the pentablocks ϕ_1 is present in Figure 2. In the pure $B_1AB_2CB_1$ terpolymers with fixed $f_A^{(1)} = f_C^{(1)} = 0.11$ and varying lengths of B blocks, the stable binary spherical phase is CsCl when the two tail B blocks are short. As the middle B_2 block is decreased, the B_2 block becomes stretched if the CsCl phase is maintained, thus inducing the A−C sphere distance l_{AC} to be shortened accompanied by shrinking the A−C spheres because of the

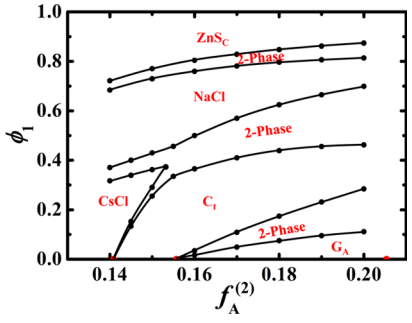

Figure 2. Phase diagram of the blend consisting of given tail-symmetric pentablock terplymers $B_1AB_2CB_3$ of $f_A^{(1)} = f_C^{(1)} = 0.11$ and $f_{B_1}^{(1)} = f_{B_3}^{(1)} = 0.34$ and symmetric ABC triblock terpolymers with varying composition, with respect to the volume fraction of the A or C block in ABC, $f_A^{(2)} = f_C^{(2)}$, and the concentration of $B_1AB_2CB_3$, ϕ_1. The length ratio between the two terpolymers is fixed as $\gamma = 0.5$, and the interaction parameters are chosen as $\chi_{AB}N = \chi_{BC}N = \chi_{AC}N = \chi N = 80$. Here the filled circles indicate the phase transition points determined by our SCFT calculations (red circles indicate these phase transition points in the pure ABC terpolymers), and the solid lines are a guide for the eyes. The label of 2-phase denotes the coexistent region of two neighboring phases.

volume conservation. In return, the size reduction of the A−C spheres raises the A/B and B/C interfacial energy. As $f_{B_2}^{(1)}$ is decreased continuously, the penalty of the interfacial energy becomes more severe. As a consequence, the highly stretched B_2 block and the increased interfacial energy lead to a phase transition, i.e., CsCl with CN = 8 transforming into NaCl with a lower CN = 6 because smaller distance l_{AC} or larger spherical size $r_{A/C}$ is permitted in the crystal lattice with a lower CN. In other words, in the crystal lattice with a lower CN, either the stretching energy of the B_2 block is released or the interfacial energy is lowered. When $f_{B_2}^{(1)}$ is decreased further, e.g., $f_{B_2}^{(1)} \leq 0.12$, the stable phase transfers from NaCl with CN = 6 to ZnS$_C$ with CN = 4.[4]

At the limit of $\phi_1 = 1$, the stable phase is the ZnS$_C$ phase, i.e., the equilibrium crystalline phase formed by the pure $B_1AB_2CB_1$ terpolymers with $f_A^{(1)} = f_C^{(1)} = 0.11$ and $f_{B_1}{}^{(1)} = f_{B_3}^{(1)} = 0.34$. At the other limit of $\phi_1 = 0$, the pure ABC triblock terpolymers with varying volume fractions $0.14 < f_A^{(2)} < 0.20$ form a phase transition sequence from the binary CsCl crystalline phase to the tetragonal cylinder phase (denoted as C$_t$) and then to the alternative gyroid phase (denoted as G$_A$). This phase sequence is consistent with the SCFT results of $\chi N = 40$ (the effective $\chi N = 80$ when considering the effect of the length ratio $\gamma = 0.5$) by Matsen.[76] The A−C sphere distance in ZnS$_C$ formed by the $B_1AB_2CB_1$ terpolymer, $l_{AC} = 1.63R_g$, is significantly smaller than that of CsCl formed by the ABC terpolymer, e.g., $l_{AC} = 2.22R_g$ for $f_A^{(2)} = 0.14$. When the ABC terpolymer is added into the $B_1AB_2CB_1$ terpolymer, the free energy penalty arising from the high stretching of the B_2 block or the increased interfacial energy is weakened. As the free energy penalty is reduced, the system tends to transfer into a new crystalline phase with a higher CN that benefits the interfacial energy in the case where the size of the A−C spheres is not significantly decreased to release the highly stretched B_2 block. As a candidate structure with a higher CN, the NaCl phase with CN = 6 that is intermediate between ZnS$_C$ and CsCl. The SCFT predicts a considerable stable region of NaCl structure below the ZnS$_C$ in the phase diagram of Figure 2. The stable region of NaCl extends to a wide range of $f_A^{(2)}$ to $f_A^{(2)} > 0.20$ where the stable phase of the pure ABC terpolymers transforms from sphere to cylinder and then to gyroid, but it becomes narrow when $f_A^{(2)}$ increases because lower content of the ABC terpolymers is allowed to maintain the low volume fractions of the A and C components for the formation of the A and C spherical domains. When ϕ_1 is decreased further, the CsCl phase exhibits a stable region at the left side of the phase diagram. In contrast, the extension of the CsCl phase region into the direction of increasing $f_A^{(2)}$ is much less than that of NaCl because at the right side high content of the ABC terpolymers make their nonspherical bulk phases more favorable in the blend. At the right side, the coexistent phase regions between the nonspherical phases, or between the nonspherical phase and the spherical phases, are also predicted. In brief, the presence of a considerable stability region of NaCl in this phase diagram suggests that the addition of simpler block copolymers into a multiblock terpolymer, e.g. ABC terpolymer, is a valid approach to make new crystalline phases beyond the bulk phase.

The length ratio γ is another crucial parameter controlling the phase behaviors in the above blend. In order to examine the effect of γ on the phase behavior of the blends, we fix the volume fractions of the ABC terpolymers as $f_A^{(2)} = f_C^{(2)} = 0.14$ and construct the phase diagram in the plane specified by γ and

DOI: 10.1021/acs.macromol.5b00529
Macromolecules 2015, 48, 3386−3394

ϕ_1. In the phase diagram shown in Figure 3, the most important feature is that there is a noticeable phase region of NaCl in the

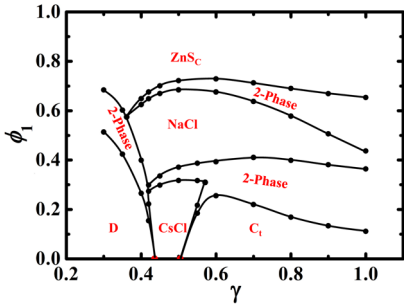

Figure 3. Phase diagram of the similar blend as that in Figure 2 but the controlling compositional parameter is replaced by the length ratio γ for $f_A^{(2)} = f_C^{(2)} = 0.14$.

central area of the phase diagram when $\gamma \geq 0.4$, and this phase region is narrowing fast when γ increases to be larger than 0.6. Indeed, the effective immiscibility of the pure ABC terpolymers is dictated by $\gamma\chi N$. With fixed $f_A^{(2)} = f_C^{(2)} = 0.14$, the bulk phase goes through the disordered phase (D) to CsCl at $\gamma = 0.436$ and then to the tetragonal cylinder phase (C_t) at $\gamma = 0.504$ when increasing γ from 0.3 to 1. At the region of $\gamma < 0.365$, the phase in the blend transforms from ZnS$_C$ to the disordered phase with a coexistent phase region between them, and only when $\gamma > 0.365$, the NaCl phase starts to appear between ZnS$_C$ and D or CsCl, as lowering the concentration of the pentablock terpolymer. However, as the length of the ABC terpolymers increasing, the domain periods as well as the domain sizes increases. As the incommensurate degree of the domain period or sizes is enlarged, the macrophase separation forming coexistent regions of two adjacent phases becomes more dominant. As a result, the expanding coexistent regions compress the microphase region of NaCl.

In the case considered above, both the block copolymers have symmetric A/C components. As a result of this symmetry, only symmetric binary crystalline phases are observed. Intuitively, an intrinsic asymmetry of the polymer architectures provides a possible way to generate asymmetric binary phases. This asymmetry could be introduced to either of the two terpolymers. To this end, we replace the symmetric ABC terpolymer by an AB diblock copolymer. For the tail-symmetric pentablock terpolymer $B_1AB_2CB_3$, the AB diblock copolymer with any composition is asymmetric from the point of view of the A/C components. The phase diagram of the blend in the $f_A^{(2)}$–ϕ_1 plane for $\gamma = 0.5$, where $f_A^{(2)}$ indicates the volume fraction of the A block of the diblock copolymer, is shown in Figure 4. For the asymmetric system, there are more candidate binary crystalline phases because of the variation of average value and asymmetry of CNs (some of them are listed in Figure 1). First we compare the free energy of as many candidate phases as possible in the canonical ensemble to screen out the more likely SCFT solutions in the grand canonical ensemble. A typical free energy comparison for a specific blend composed of the multiblock terpolymer and the AB diblock copolymer with a given volume fraction $f_A^{(2)} = 0.16$ is given in Figure 5, where 10 binary spherical phases plus two single spherical phases are considered. In the canonical ensemble, the stable phase sequence for increasing ϕ_1 is bcc, SnI_4 with the space group $I\bar{4}2m$ and CNs = (4, 1) ($\overline{CN} = 8/5$), Cu_2O with the space group $Pn3m$ and CNs = (4, 2) ($\overline{CN} = 8/3$), and ZnS$_C$ with

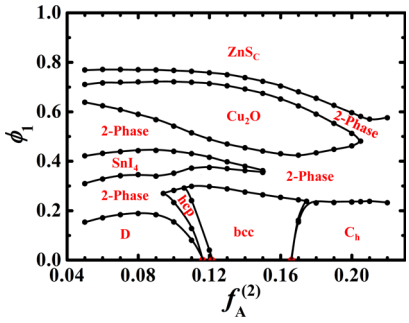

Figure 4. Phase diagram in the $f_A^{(2)}$–ϕ_1 plane for the binary blend of given tail-symmetric $B_1AB_2CB_3$ terpolymers with $f_A^{(1)} = f_C^{(1)} = 0.11$ and $f_{B_1}^{(1)} = f_{B_3}^{(1)} = 0.34$, and AB diblock copolymers, for a fixed length ratio $\gamma = 0.5$.

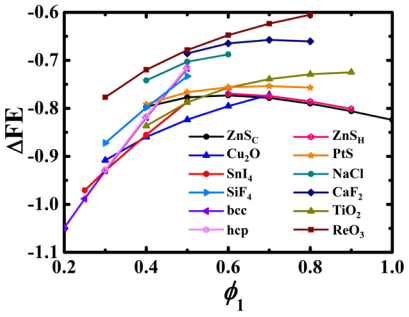

Figure 5. Free energy comparison of candidate phases for the similar blend as that in Figure 4 but with a given $f_A^{(2)} = 0.16$.

equal CN = 4. Apparently, the average value of CNs of the three binary phases in this phase sequence increases gradually as increasing the concentration of the pentablock terpolymers. It is surprising that the two binary phases with unequal CNs are not observed as stable in pure tail-asymmetric $B_1AB_2CB_3$ terpolymers.[4] This implies that blending the specially designed multiblock terpolymers with simpler block copolymers provides a feasible way to fabricate new crystalline phases beyond those formed by the pure multiblock terpolymers.

In Figure 4, two new binary crystalline phase Cu_2O and SnI_4 are predicted as stable phases. Compared with the lattice of ZnS$_C$, the C spheres (blue) with higher CN in Cu_2O are arranged on the bcc lattice instead of the face centered cubic (fcc) lattice, while A spheres are placed at the similar quarter position on the diagonals. Moreover, Cu_2O has lower unequal CNs. As a consequence, the B blocks in Cu_2O are more nonuniformly stretched than in ZnS$_C$, especially around the center of each face of the cubic unit. The majority B blocks of the AB diblock copolymers can freely reach these further space because they are significantly longer than the tail B blocks of the $B_1AB_2CB_3$ terpolymers, for example, $\gamma f_B^{(2)} N = 0.42N$ for $\gamma = 0.5$ and $f_A^{(2)} = 0.16$ is longer than $f_{B_1}^{(1)} N = f_{B_3}^{(1)} N = 0.34N$. Thus, their addition favors stabilizing the new binary phase Cu_2O. In Figure 6, the aggregation of the B blocks of AB for $f_A^{(2)} = 0.16$ and $\gamma = 0.5$ is demonstrated by its isosurface plots. As increasing $f_A^{(2)}$ or reducing $f_B^{(2)}$, the ability of stabilizing Cu_2O of the AB diblock copolymers is weakened, and thereby the stability region of Cu_2O is invaded by that of ZnS$_C$. In addition, as entering the cylinder phase region of AB, the mismatch of domain shapes increases the tendency of macrophase separations that also narrows the Cu_2O phase region. Note that the stable phase SnI_4 in the phase sequence of the

DOI: 10.1021/acs.macromol.5b00529
Macromolecules 2015, 48, 3386−3394

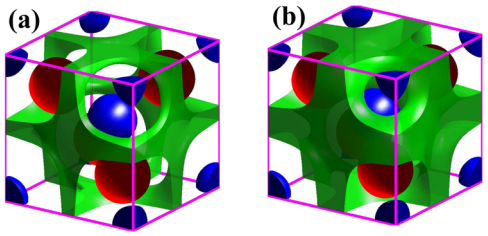

Figure 6. Density isosurface plots of the Cu_2O crystalline phase formed in the binary blend of the tail-symmetric $B_1AB_2CB_1$ terpolymer and the AB diblock copolymer with a typical group of parameters inside the phase region of Cu_2O in Figure 4, $f_A^{(2)} = 0.16$, $\gamma = 0.5$, and $\phi_1 \approx 0.56$. The red and blue colors represent the A- and C-rich domains, respectively, while the green color indicate the B block density of the AB diblock copolymer alone. Two isosurfaces of the B blocks with two different densities of 0.53 and 0.50 are plotted in (a) and (b), respectively. Large green domains in (b) than in (a) suggests that the B blocks of the AB diblock copolymer aggregate inside the green domains far from those spherical surfaces.

canonical ensemble does not appear for $f_A^{(2)} > 0.15$ in the phase diagram calculated in the grand canonical ensemble though it is stable in the canonical-ensemble calculation. The reason is that the SnI_4 phase is simply replaced by the coexistent region of the Cu_2O and bcc phases because the free energy of the SnI_4 phase is higher than that of the coexistent two phases (i.e., the linear combination of the free energy of the two phases). Interestingly, SnI_4 exhibits a narrow stable region between $\phi_1 = 0.3$ and 0.45 when $f_A^{(2)} < 0.15$. The SnI_4 phase can be derived from Cu_2O by removing the C sphere at the cubic center. Accordingly, the tail B-blocks of the pentablock terpolymers in SnI_4 are more severely stretched to reach the space at the cubic center, and the asymmetry between the A and C components is necessary to be larger. The two shortcomings are overcome by the addition of higher concentration of AB diblock copolymers with longer B block.

In Figure 7, we calculate the phase diagram of the second blend with respect to the length ratio γ of the two polymers and

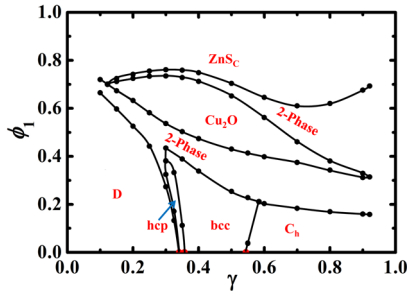

Figure 7. Phase diagram in the $\gamma-\phi_1$ plane of the similar blend as that in Figure 4 for $f_A^{(2)} = 0.16$.

ϕ_1 for a fixed $f_A^{(2)} = 0.16$. The most important feature is the presence of a considerable phase region of the Cu_2O phase in the central region that vanishes at two limits, i.e., $\gamma < 0.1$ or $\gamma > 0.9$, respectively. In the region of short AB diblock copolymers, the disordered phase occupies the phase region of low concentrations of the multiblock terpolymers, compressing the Cu_2O phase region, whereas for long AB diblock copolymers, the coexistent phase regions expands to reduce the Cu_2O phase region. When $0.3 < \gamma < 0.6$, the Cu_2O phase exhibits a considerably wide stability region.

In the previous two blending systems, symmetric ABC terpolymers and AB diblock copolymers with varying compositions and lengths are added into the given tail-symmetric $B_1AB_2CB_1$ terpolymers to fabricate new symmetric and asymmetric crystalline phases, respectively. In the third example, we replace the tail-symmetric $B_1AB_2CB_1$ terpolymer with a tail-asymmetric tetrablock terpolymer AB_2CB_3 with fixed $f_A^{(1)} = f_C^{(1)} = 0.09$ and $f_{B_2}^{(1)} = 0.20$, whose self-assembly can form the binary crystal phase ReO_3 with unequal low CNs = (6, 2) ($\overline{CN} = 3$), and then mix it with the symmetric ABC terpolymer to examine the formation of various binary crystal phases. The phase diagrams in the $f_A^{(2)}-\phi_1$ plane with fixed $\gamma = 0.5$ and in the $\gamma-\phi_1$ plane with fixed $f_A^{(2)} = f_C^{(2)} = 0.14$ are present in Figures 8 and 9, respectively. In Figure 8, as adding the ABC

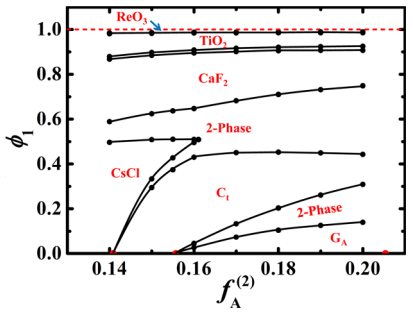

Figure 8. Phase diagram in the $f_A^{(2)}-\phi_1$ plane of the blend composed of tail-asymmetric AB_2CB_3 tetrablock terplymers with $f_A^{(1)} = f_C^{(1)} = 0.09$ and $f_{B_2}^{(1)} = 0.20$ and symmetric ABC triblock terpolymers with varying volume fraction $f_A^{(2)}$. The length ratio of the two terpolymers is fixed as $\gamma = 0.5$. With these fixed parameters, the pure tetrablock terplymer forms the binary crystalline phase of ReO_3.

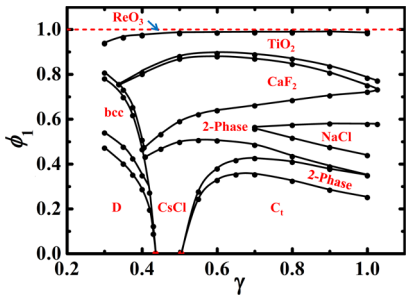

Figure 9. Phase diagram in the $\gamma-\phi_1$ plane of the similar blend as that in Figure 8 for fixed $f_A^{(2)} = f_C^{(2)} = 0.14$.

terpolymers, the binary phase transforms from ReO_3 to TiO_2 with CNs = (6, 3) ($\overline{CN} = 4$), to CaF_2 with CNs = (8, 4) ($\overline{CN} = 16/3$), and then to the bulk phases of the pure added terpolymers. The average value of CNs follows an increasing tendency when the blend varies from the pure pentablock terpolymer to the pure ABC terpolymer. In other words, two binary crystalline phases different from that formed in the pure tetrablock terpolymers are generated by adding the simpler ABC terpolymers. Specifically, the addition of a tiny amount of the ABC terpolymers induces the stable phase to transform from ReO_3 to TiO_2.

In the phase diagram of Figure 9, the two new binary phases of TiO_2 and CaF_2 exhibit their corresponding stable regions. The TiO_2 phase region expands a wide space with a minimal width at around $\gamma = 0.6$, and it does not terminate in the considered range of parameters $0.3 \leq \gamma \leq 1.0$. Because the main

DOI: 10.1021/acs.macromol.5b00529
Macromolecules 2015, 48, 3386−3394

task of our work is to demonstrate that adding simpler block copolymers into designed multiblock terpolymers is a useful scheme to yield more binary crstalline phases, here we do not expand our parameter space further. In contrast to TiO_2, the CaF_2 phase has a wider region in the parameter range of $0.4 < \gamma < 0.7$ but terminates at two sides. In addition to the binary crystal phases with unequal CNs, in the right side of the phase diagram there is a small region of the binary NaCl phase with equal CNs differing from the CsCl phase formed in the pure ABC terpolymers. This implies that the symmetric binary phase can become stable in the blend containing A/C architecture asymmetric terpolymers.

■ CONCLUSIONS

In summary, we have obtained phase diagrams of three binary blends composed of tail symmetric or asymmetric multiblock terpolymers and ABC triblock terpolymers or AB diblock copolymers using SCFT. The results clearly demonstrated that the addition of simpler block copolymers into complex multiblock terpolymers resulted in the formation of new binary crystalline phases which are not available from the pure multiblock terpolymers. In the first blend composed of given tail-symmetric $B_1AB_2CB_3$ terpolymers and symmetric ABC terpolymers with varying composition or chain length, besides the binary phases of ZnS_C and CsCl that are the stable phases of the two pure terpolymers, the binary phase of NaCl has a considerable stable phase region. More interestingly, in the second blend where the symmetric ABC terpolymer of the first blend is replaced with the AB diblock copolymers, two novel asymmetric binary crystalline phases, Cu_2O and SnI_4, appear with notable stable phase regions. In particular, the two phases have not been identified as stable phase in pure asymmetric $B_1AB_2CB_3$ terpolymers.[4] In these two phases, the majority B blocks of the AB diblock copolymers which are significantly longer than the tail B blocks of the pentablock terpolymers are preferentially located in the further space to reduce the stretching of the tail B blocks and thus to facilitate stabilizing the two new phases. Appropriate composition and chain length for the AB copolymers are required to stabilize the Cu_2O and SnI_4 phases because of possible macrophase separations leading to the coexistent phase regions of two phases and thus narrowing their phase regions. In the third blend composed of tail-asymmetric tetrablock terpolymers AB_2CB_3 and symmetric ABC terpolymers, predicted stable binary phases differing from those formed in the two pure terpolymers include two asymmetric binary phases of TiO_2 and CaF_2 and one symmetric binary phase of NaCl. Our results demonstrate that blending simpler block copolymers with specially designed complex multiblock terpolymers is a useful scheme to fabricate binary crystalline phases that are different from those formed in the pure terpolymers. Although in practice it is difficult for experimentalists to obtain these interesting structures in these specific block copolymer samples with a restricted set of parameters, our work demonstrates a valid blending scheme which offers opportunities for the fabrication of various binary crystalline phases with one complex multiblock terpolymer in a relative low cost and therefore might motivate relative experimental studies.

■ AUTHOR INFORMATION

Corresponding Author

*Phone +86 21 65643579; Fax +86 21 65640293; e-mail weihuali@fudan.edu.cn (W.L.).

Notes

The authors declare no competing financial interest.

■ ACKNOWLEDGMENTS

This work was supported by the National Natural Science Foundation of China (Grants 21322407 and 21174031), the National High Technology Research and Development Program of China (863 Grant 2008AA032101), and the National Science Foundation for Postdoctoral Scientists of China (Grant 2014M560289). A.-C.S. acknowledges the support from the Natural Science and Engineering Research Council (NSERC) of Canada.

■ REFERENCES

(1) Bates, F. S.; Fredrickson, G. H. *Phys. Today* **1999**, *52*, 32−38.
(2) Guo, Z. J.; Zhang, G. J.; Qiu, F.; Zhang, H. D.; Yang, Y. L.; Shi, A.-C. *Phys. Rev. Lett.* **2008**, *101*, 028301.
(3) Xu, W. Q.; Jiang, K.; Zhang, P. W.; Shi, A.-C. *J. Phys. Chem. B* **2013**, *117*, 5296−5305.
(4) Xie, N.; Liu, M.; Deng, H.; Li, W.; Qiu, F.; Shi, A.-C. *J. Am. Chem. Soc.* **2014**, *136*, 2974−2977.
(5) Matsen, M. W.; Schick, M. *Phys. Rev. Lett.* **1994**, *72*, 2660−2663.
(6) Tyler, C.; Morse, D. *Phys. Rev. Lett.* **2005**, *94*, 208302.
(7) Matsen, M. W. *Macromolecules* **2012**, *45*, 2161−2165.
(8) Lee, S.; Bluemle, M. J.; Bates, F. S. *Science* **2010**, *330*, 349−353.
(9) Lee, S.; Leighton, C.; Bates, F. S. *Proc. Natl. Acad. Sci. U. S. A.* **2014**, *111*, 17723−17731.
(10) Xie, N.; Li, W. H.; Qiu, F.; Shi, A.-C. *ACS Macro Lett.* **2014**, *3*, 906−910.
(11) Kang, Y.; Walish, J. J.; Gorishnyy, T.; Thomas, E. L. *Nat. Mater.* **2007**, *6*, 957−960.
(12) Deng, T.; Chen, C.; Honeker, C.; Thomas, E. L. *Polymer* **2003**, *44*, 6549−6553.
(13) Urbas, A. M.; Maldovan, M.; DeRege, P.; Thomas, E. L. *Adv. Mater.* **2002**, *14*, 1850−1853.
(14) Hashimoto, T.; Tsutsumi, K.; Funaki, Y. *Langmuir* **1997**, *13*, 6869−6872.
(15) Crossland, E. J. W.; Kamperman, M.; Nedelcu, M.; Ducati, C.; Wiesner, U.; Smilgies, D. M.; Toombes, G. E. S.; Hillmyer, M. A.; Ludwigs, S.; Steiner, U.; Snaith, H. J. *Nano Lett.* **2009**, *9*, 2807−2812.
(16) Hsueh, H. Y.; Huang, Y. C.; Ho, R. M.; Lai, C. H.; Makida, T.; Hasegawa, H. *Adv. Mater.* **2011**, *23*, 3041−3046.
(17) Ruiz, R.; Kang, H.; Detcheverry, F. A.; Dobisz, E.; Kercher, D. S.; Albrecht, T. R.; de Pablo, J. J.; Nealey, P. F. *Science* **2008**, *321*, 936−939.
(18) Kim, S. O.; Solak, H. H.; Stoykovich, M. P.; Ferrier, N. J.; de Pablo, J. J.; Nealey, P. F. *Nature* **2003**, *424*, 411−414.
(19) Yang, X.; Xiao, S.; Liu, C.; Pelhos, K.; Minor, K. *J. Vac. Sci. Technol., B* **2004**, *22*, 3331−3334.
(20) Griffiths, R. A.; Williams, A.; Oakland, C.; Roberts, J.; Vijayaraghavan, A.; Thomson, T. *J. Phys. D: Appl. Phys.* **2013**, *46* (503001), 1−29.
(21) Stoykovich, M. P.; Müller, M.; Kim, S. O.; Solak, H. H.; Edwards, E. W.; de Pablo, J. J.; Nealey, P. F. *Science* **2005**, *308*, 1442−1446.
(22) Stoykovich, M. P.; Kang, H.; Daoulas, K. C.; Liu, G.; Liu, C.-C.; de Pablo, J. J.; Müller, M.; Nealey, P. F. *ACS Nano* **2007**, *1*, 168−175.
(23) Chang, J.-B.; Choi, H. K.; Hannon, A. F.; Alexander-Katz, A.; Ross, C. A.; Berggren, K. K. *Nat. Commun.* **2014**, *5*, 3305.
(24) Park, M.; Harrison, C.; Chaikin, P. M.; Register, R. A.; Adamson, D. H. *Science* **1997**, *276*, 1401−1404.
(25) Chan, V. Z. H.; Hoffman, J.; Lee, V. Y.; Iatrou, H.; Avgeropoulos, A.; Hadjichristidis, N.; Miller, R. D.; Thomas, E. L. *Science* **1999**, *286*, 1716−1719.
(26) Thurn-Albrecht, T.; Schotter, J.; Kästle, G. A.; Emley, N.; Shibauchi, T.; Krusin-Elbaum, L.; Guarini, K.; Black, C. T.; Tuominen, M. T.; Russell, T. P. *Science* **2000**, *290*, 2126−2129.

DOI: 10.1021/acs.macromol.5b00529
Macromolecules 2015, 48, 3386−3394

(27) Lopes, W. A.; Jaeger, H. M. *Nature* **2001**, *414*, 735−738.
(28) McConnell, G. A.; Gast, A. P.; Huang, J. S.; Smith, S. D. *Phys. Rev. Lett.* **1993**, *71*, 2102−2105.
(29) Balagurusamy, V. S. K.; Ungar, G.; Percec, V.; Johansson, G. *J. Am. Chem. Soc.* **1997**, *119*, 1539−1555.
(30) Percec, V.; Ahn, C. H.; Ungar, G.; Yeardley, D. J. P.; Möller, M.; Sheiko, S. S. *Nature* **1998**, *391*, 161−164.
(31) Ziherl, P.; Kamien, R. D. *Phys. Rev. Lett.* **2000**, *85*, 3528−3531.
(32) Ungar, G.; Liu, Y. S.; Zeng, X. B.; Percec, V.; Cho, W. D. *Science* **2003**, *299*, 1208−1211.
(33) Zeng, X. B.; Ungar, G.; Liu, Y. S.; Percec, V.; Dulcey, A. E.; Hobbs, J. K. *Nature* **2004**, *428*, 157−160.
(34) Peterca, M.; Percec, V. *Science* **2010**, *330*, 333−334.
(35) Huang, C.-I.; Yang, L.-F. *Macromolecules* **2010**, *43*, 9117−9125.
(36) Spencer, R. K. W.; Wickham, R. A. *Soft Matter* **2013**, *9*, 3373−3382.
(37) Thomson, W. *Philos. Mag. Lett.* **1887**, *24*, 503.
(38) Weaire, D.; Phelan, R. *Philos. Mag. Lett.* **1994**, *69*, 107−110.
(39) Bates, F. S.; Hillmyer, M. A.; Lodge, T. P.; Bates, C. M.; Delaney, K. T.; Fredrickson, G. H. *Science* **2012**, *336*, 434−440.
(40) Milner, S. T. *Macromolecules* **1994**, *27*, 2333−2335.
(41) Beyer, F. L.; Gido, S. P.; Velis, G.; Hadjichristidis, N.; Tan, N. B. *Macromolecules* **1999**, *32*, 6604−6607.
(42) Grason, G. M.; DiDonna, B. A.; Kamien, R. D. *Phys. Rev. Lett.* **2003**, *91*, 58304.
(43) Grason, G. M.; Kamien, R. D. *Macromolecules* **2004**, *37*, 7371−7380.
(44) Zhang, J.; Sides, S.; Bates, F. S. *Macromolecules* **2012**, *45*, 256−265.
(45) Zhang, J.; Bates, F. S. *J. Am. Chem. Soc.* **2012**, *134*, 7636−7639.
(46) Hashimoto, T.; Koizumi, S.; Hasegawa, H.; Izumitani, T.; Hyde, S. T. *Macromolecules* **1992**, *25*, 1433−1439.
(47) Bodycomb, J.; Yamaguchi, D.; Hashimoto, T. *Macromolecules* **2000**, *33*, 5187−5197.
(48) Matsushita, Y.; Noro, A.; Iinuma, M.; Suzuki, J.; Ohtani, H.; Takano, A. *Macromolecules* **2003**, *36*, 8074−8077.
(49) Huang, Y. Y.; Hsu, J. Y.; Chen, H. L.; Hashimoto, T. *Macromolecules* **2007**, *40*, 3700−3707.
(50) Whitmore, M. D.; Noolandi, J. *Macromolecules* **1985**, *18*, 2486−2497.
(51) Matsen, M. W. *Phys. Rev. Lett.* **1995**, *74*, 4225−4228.
(52) Matsen, M. W. *Macromolecules* **1995**, *28*, 5765−5773.
(53) Matsen, M. W. *Macromolecules* **2003**, *36*, 9647−9657.
(54) Epps, T. H.; Chatterjee, J.; Bates, F. S. *Macromolecules* **2005**, *38*, 8775−8784.
(55) Tureau, M. S.; Rong, L.; Hsiao, B. S.; Epps, T. H. *Macromolecules* **2010**, *43*, 9039−9048.
(56) Abetz, V.; Jiang, S. M. *e-Polym.* **2004**, *54*, 1−9.
(57) Yamauchi, K.; Akasaka, S.; Hasegawa, H.; Iatrou, H.; Hadjichristidis, N. *Macromolecules* **2005**, *38*, 8022−8027.
(58) Matsushita, Y.; Hayashida, K.; Takano, A. *Macromol. Rapid Commun.* **2010**, *31*, 1579−1587.
(59) Goldacker, T.; Abetz, V. *Macromol. Rapid Commun.* **1999**, *20*, 415−418.
(60) Yamaguchi, D.; Hashimoto, T. *Macromolecules* **2001**, *34*, 6495−6505.
(61) Li, W. H.; Müller, M. *Annu. Rev. Chem. Biomol. Eng.* **2015**, DOI: 10.1146/annurev-chembioeng-061114-123209.
(62) Shi, A.-C. *Developments in Block Copolymer Science and Technology*; John Wiley & Sons, Ltd.: New York, 2004; pp 265−293.
(63) Fredrickson, G. H. *The Equilibrium Theory of Inhomogeneous Polymers*; Oxford University Press: New York, 2006.
(64) Fredrickson, G. H.; Helfand, E. *J. Chem. Phys.* **1987**, *87*, 697−705.
(65) Li, W. H.; Qiu, F.; Shi, A.-C. *Macromolecules* **2012**, *45*, 503−509.
(66) Liu, M. J.; Li, W. H.; Qiu, F.; Shi, A.-C. *Macromolecules* **2012**, *45*, 9522−9530.
(67) Janert, P. K.; Schick, M. *Macromolecules* **1998**, *31*, 1109−1113.
(68) Wu, Z. Q.; Li, B. H.; Jin, Q. H.; Ding, D. T.; Shi, A.-C. J. *Phys. Chem. B* **2010**, *114*, 15789−15798.
(69) Rasmussen, K. O.; Kalosakas, G. *J. Polym. Sci., Part B: Polym. Phys.* **2002**, *40*, 1777−1783.
(70) Tzeremes, G.; Rasmussen, K. O.; Lookman, T.; Saxena, A. *Phys. Rev. E* **2002**, *65*, 041806.
(71) Thompson, R. B.; Rasmussen, K. O.; Lookman, T. *J. Chem. Phys.* **2004**, *120*, 31−34.
(72) Stasiak, P.; Matsen, M. W. *Eur. Phys. J. E* **2011**, *34*, 110.
(73) Cochran, E. W.; Garcia-Cervera, C. J.; Fredrickson, G. H. *Macromolecules* **2006**, *39*, 2449−2451.
(74) Ranjan, A.; Qin, J.; Morse, D. C. *Macromolecules* **2008**, *41*, 942−954.
(75) Xu, Y. C.; Li, W. H.; Qiu, F.; Zhang, H. D.; Yang, Y. L.; Shi, A. C. *J. Polym. Sci., Part B: Polym. Phys.* **2010**, *48*, 1101−1109.
(76) Matsen, M. W. *J. Chem. Phys.* **1998**, *108*, 785−796.

DOI: 10.1021/acs.macromol.5b00529
Macromolecules 2015, 48, 3386−3394